Prediction of scour depth around bridge piers using self-adaptive extreme learning machine

Isa Ebtehaj, Ahmed M. A. Sattar, Hossein Bonakdari and Amir Hossein Zaji

ABSTRACT

Accurate prediction of pier scour can lead to economic design of bridge piers and prevent catastrophic incidents. This paper presents the application of self-adaptive evolutionary extreme learning machine (SAELM) to develop a new model for the prediction of local scour around bridge piers using 476 field pier scour measurements with four shapes of piers: sharp, round, cylindrical, and square. The model network parameters are optimized using the differential evolution algorithm. The best SAELM model calculates the scour depth as a function of pier dimensions and the sediment mean diameter. The developed SAELM model had the lowest error indicators when compared to regression-based prediction models for root mean square error (*RMSE*) (0.15, 0.65, respectively) and mean absolute relative error (*MARE*) (0.50, 2.0, respectively). The SAELM model was found to perform better than artificial neural networks or support vector machines on the same dataset. Parametric analysis showed that the new model predictions are influenced by pier dimensions and bed-sediment size and produce similar trends of variations of scour-hole depth as reported in literature and previous experimental measurements. The prediction uncertainty of the developed SAELM model is quantified and compared with existing regression-based models and found to be the least, ±0.03 compared with ±0.10 for other models.

Key words | artificial intelligence, pier scour, SAELM, self-adaptive extreme learning machine, sensitivity analysis

Isa Ebtehaj
Hossein Bonakdari (corresponding author)
Amir Hossein Zaji
Department of Civil Engineering,
Razi University,
Kermanshah,
Iran
E-mail: *bonakdari@yahoo.com*

Ahmed M. A. Sattar
Department of Irrigation & Hydraulics,
Cairo University,
Giza,
Egypt

INTRODUCTION

The presence of a bridge structure in a flow channel inevitably involves a significant change to the flow pattern, which in turns induces the formation of a scour hole at the piers. Bridge scour is the result of the erosive action of flowing water excavating and carrying away material from the bed and banks of streams and from around the piers and abutments of bridges. The scouring effect of the flowing water around bridge piers is a common issue that engineers have to face both at the design and maintenance stages. Therefore, safe and economical design of the bridge piers requires accurate prediction of the maximum scour depth around their foundations. Underestimation may lead to bridge failure and overestimation unnecessarily increases construction costs.

Investigations into the scour around bridge piers were initiated in the 1950s. Several researchers have carried out experimental investigations and proposed traditional equations for the prediction of scour depth around piers (e.g., Laursen & Toch 1956; Melville & Sutherland 1998; Richardson & Davis 2001). Their proposed formulae were based largely on dimensional analyses on small-scale laboratory experiments (e.g., Simons & Senturk 1992) under simplified conditions presuming non-cohesive and uniform bed materials and constant-depth and stable water-flow conditions. Kafi & Alam (1995) and Mueller & Wagner (2005) studied various developed scour relations and came to the conclusion that the accuracy of the scour prediction equations can be increased if field scour data were used to

doi: 10.2166/hydro.2016.025

calibrate the developed relations. This urged many researchers to develop scour prediction equations using field data. Froehlich (1988) utilized 83 field observations to obtain a regression-based scour model. Kafi & Alam (1995) collected 40 field data for bridge pier scour and developed an empirical based relation. Using the same 40 datasets of Kafi & Alam (1995), Ab Ghani & Nalluri (1996), Yahaya & Ab Ghani (1999), Yahaya *et al.* (2002) proposed new equations for scour depth prediction.

Multiple factors influence scour depth such as channel-bed composition, flow velocity and skewness of the pier to the approach flow. Moreover, the relationship between scour depth and each of its influencing factors is complex and potentially nonlinear. Furthermore, the input data used to represent natural phenomena are typically imprecise and qualified. Capturing these complex nonlinear relationships and handling the uncertainties inherent in input data often exceeds the capabilities of the traditional regression-based models. This was confirmed by Gaudio *et al.* (2013) who studied various regression-based equations and found that their sensitivity to various input parameters varies over a wide range. This causes uncertainty in predictions and significant error in scour depth as a result of a small error in one of the input parameters. More accurate estimation of pier scour depth plays an important role in the design of many types of scour countermeasures (Gaudio *et al.* 2010; Tafarojnoruz *et al.* 2010).

The use of alternative soft computing tools has been recently devised to solving problems involving complex nonlinear relationships between various parameters. These include artificial neural networks (ANN) (Kazeminezhad & Etemad-Shahidi 2010), radial basis functions (RBF) (Vojinovic *et al.* 2003), genetic programming (Babovic 2000, 2009), support vector machines (SVM) (Babovic *et al.* 2000; Yu *et al.* 2004), group method of data handling (Najafzadeh & Sattar 2015), adaptive neuro fuzzy inference system (Ebtehaj & Bonakdari 2014; Ebtehaj *et al.* 2015), model tree (Etemad-Shahidi *et al.* 2015), and gene expression programming (Sattar 2014; El-Hakeem & Sattar 2015).

Cao *et al.* (2012) developed an intelligent self-adaptive evolutionary extreme learning method (SAELM) that is capable of calculating the optimum weights in neural network's hidden layers. This results in high performance capacity and fast training for large datasets with complex nonlinear variables. The SAELM method has been successfully used in Cao & Xiong (2014), Luo *et al.* (2014), Zong & Huang (2014), and Lian *et al.* (2014). However, despite having many desirable features and high performance, the authors have not identified any application of the SAELM to the prediction of pier scour depth.

This study aims at applying the SAELM algorithm in a novel application, to develop a new model for the prediction of pier scour depth that provides more accurate predictions and thus safer and more economic bridge pier design. This study is intended to overcome the shortcomings in previous models by: using a large comprehensive field dataset covering various shapes of piers; using SAELM algorithm to overcome disadvantages in previous ANN applications; provide a simple model showing the relationship between various control variables and the physics of the process; and assess the uncertainty in developed model prediction.

Initially, a brief overview on the pier scour process is presented in addition to presenting the available traditional regression-based models. Then, the SAELM model is presented in brief, followed by the collected dataset with various input parameters. The developed SAELM model is then validated against the traditional regression-based models and two well known soft computing methods, ANN and SVM.

BRIDGE PIER LOCAL SCOUR AND AVAILABLE PREDICTION MODELS

The flow structure around a pier is complex, three-dimensional, and unsteady in nature with a combination of horseshoe and wake vortices as shown in Figure 1, when the approaching flow velocity encounters the bridge pier, its magnitude changes. The velocity magnitude decreases in the vertical direction starting from a maximum value at the surface and a zero value at the lower face of the pier. This creates a downward pressure gradient on the pier face that causes an increase in the downward motion (Dey *et al.* 1995). This downward flow initiates the scour, forming a small 'ring' of scoured material (Guo 2012). Afterwards, the flow moves down and around the pier forming the horseshoe vortex at the heel of the pier, which is trapped by the formed 'ring' causing rapid removal of sediment from the bottom of the pier. The circulation in the scour hole continues to remove bed material until reaching an equilibrium state, where no more sediment is removed (Chiew 1984). This equilibrium state is defined as

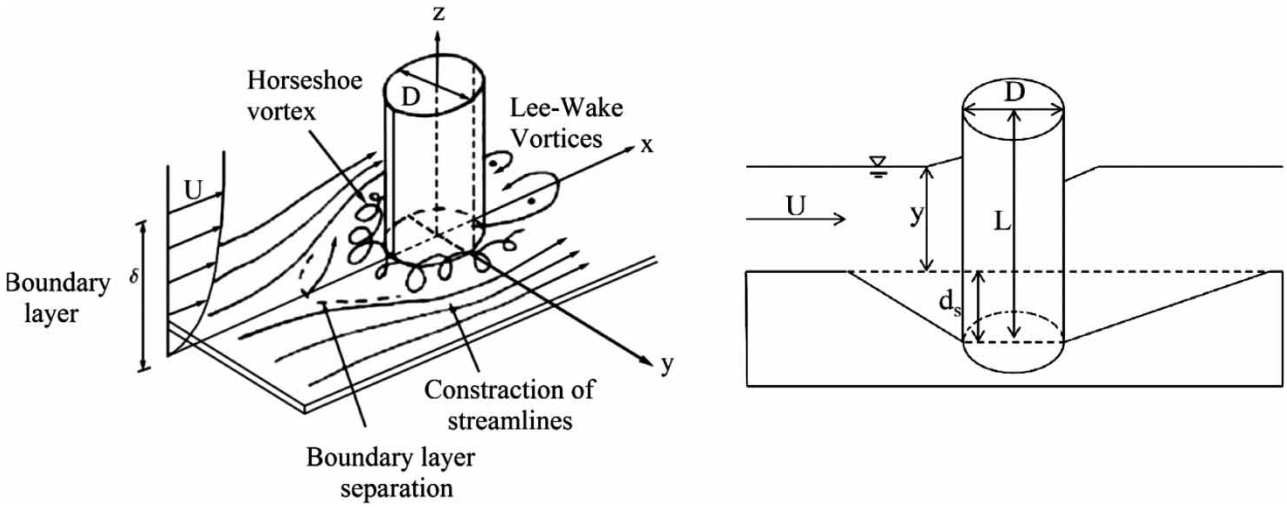

Figure 1 | Local scour and flow around cylindrical pier.

the state where the shear stress caused by the horseshoe vortex is equal to or more than the critical shear stress of bed material at the pier location. This equilibrium scour depth usually takes a long time to form in practice, and when it is reached, some sediment removal might take place. However, the amount of sediment removed does not affect the formed scour hole. Once the equilibrium is reached and the scour hole is formed, its upstream slope tends to be close to the angle of repose of the sand (Williams *et al.* 2013).

Chiew (1984) has categorized the majority of variables affecting pier scour depth into five groups. These include: fluid properties, time, flow properties, pier characteristics and sediment characteristics. These effective parameters can be presented as follows:

$$d_s = f(g, L, y, d_{50}, \sigma, D, U) \tag{1}$$

where d_s is the local scour depth, g is the gravitational acceleration, L is the pier length, y is the flow depth, d_{50} is the median diameter of particle size, σ is the standard deviation of the bed grain size, U is the average velocity and D is the pier width. These variables can be reduced to a set of non-dimensional parameters as (Williams *et al.* 2013):

$$\frac{d_s}{y} = f\left(\frac{L}{y}, \frac{d_{50}}{y}, \frac{D}{y}, Fr, \sigma\right) \tag{2}$$

where Fr is the Froude number.

Various combinations of the above parameters have been utilized by researchers to develop empricial equations for the prediction of pier scour hole depth. Table 1 shows some traditional regression-based development models that have been widely used in the past half-century.

SELF-ADAPTIVE EXTREME LEARNING MACHINE

The SAELM method is comprised of two integrated components, the extreme learning machine (ELM) regression method and the self-adaptive version of the differential evolution (DE). In the following section, a brief overview is given for the ELM and DE, interested readers can find more details in Cao *et al.* (2012). Following the brief on both components, their integration within the SAELM procedure is discussed.

Table 1 | Available regression-based scour hole prediction models

Author	Equation
Laursen & Toch (1956)	$d_s/y = 1.35(D/y)^{0.7}$
Shen *et al.* (1969)	$d_s/y = 3.4(Fr^{0.67})(D/y)^{0.67}$
Johnson (1992)	$d_s/y = 2.02(Fr^{0.21})(D/y)^{0.98}(\sigma^{-0.98})$
Richardson & Davis (2001)	$d_s/y = 2.6(D/y)^{0.65}(Fr^{0.43})$

Extreme learning machine

The ELM neural network, which is introduced by Huang *et al.* (2006), is presented in this section. Because of the high ability of the ELM method in simulating the nonlinear problems, recently this method is widely used in different engineering problems. In the ELM procedure, the least-square training algorithm is used in order to develop a single-layer forward network as shown in Figure 2. The ELM is constructed from three layers: an input layer, a hidden layer, and an output layer. In the ELM learning procedure, the hidden layer's weights (w_{ij}) are selected randomly, so that only the output layer's weights (β_{jk}) are determined in the training procedure (Huang *et al.* 2012). Thus, ELM is a rapid training neural network that is very suitable for the applicable problems. According to Figure 2, ELM structure has a full connection between the input-to-hidden and hidden-to-output layer. The input layer has n neurons that are equal to the number of input variables of the considered problem. Similarly, the output layer has m neurons that are equal to the number of output variables of the considered problem. Regarding the hidden layer's neuron number, they are determined by a trial and error procedure considering the complexity of the problem.

If we consider l neurons in the hidden layer (where l is the number of neurons in the hidden layer), the input-to-hidden weight matrix is obtained from $\mathrm{w} = [w_{ij}]_{n\times l}$, where w_{ij} is a coefficient that connected the ith neuron of the input layer to the jth neuron of the hidden layer. The hidden-to-output layer matrix is obtained $\beta = [\beta_{jk}]_{l\times m}$, where β_{jk} is a coefficient that connecting the jth neuron of the hidden layer to the kth neuron of the output layer. In addition, the input (X) and target (Y) matrices of the problem are considered as $\mathrm{X} = [x_{ij}]_{n\times Q}$ and $\mathrm{Y} = [y_{ij}]_{m\times Q}$ where Q is the input samples number. The results of the ELM are shown by $\mathrm{T} = (\mathrm{t}_1, \mathrm{t}_2, \ldots, \mathrm{t}_Q)_{\mathrm{m\times Q}}$. Each output is defined as:

$$\mathrm{t}_j = \begin{bmatrix} t_{1j} \\ t_{2j} \\ \vdots \\ t_{mj} \end{bmatrix}_{m\times 1} = \begin{bmatrix} \sum_{i=1}^{l} \beta_{i1} g(\mathrm{w}_i \mathrm{x}_i + b_i) \\ \sum_{i=1}^{l} \beta_{i2} g(\mathrm{w}_i \mathrm{x}_i + b_i) \\ \vdots \\ \sum_{i=1}^{l} \beta_{im} g(\mathrm{w}_i \mathrm{x}_i + b_i) \end{bmatrix}_{m\times 1} ,(j = 1, 2, \ldots, Q) \tag{3}$$

In this equation, $g(x)$ is the neural network activation function. In this study, the sigmoid activation function is

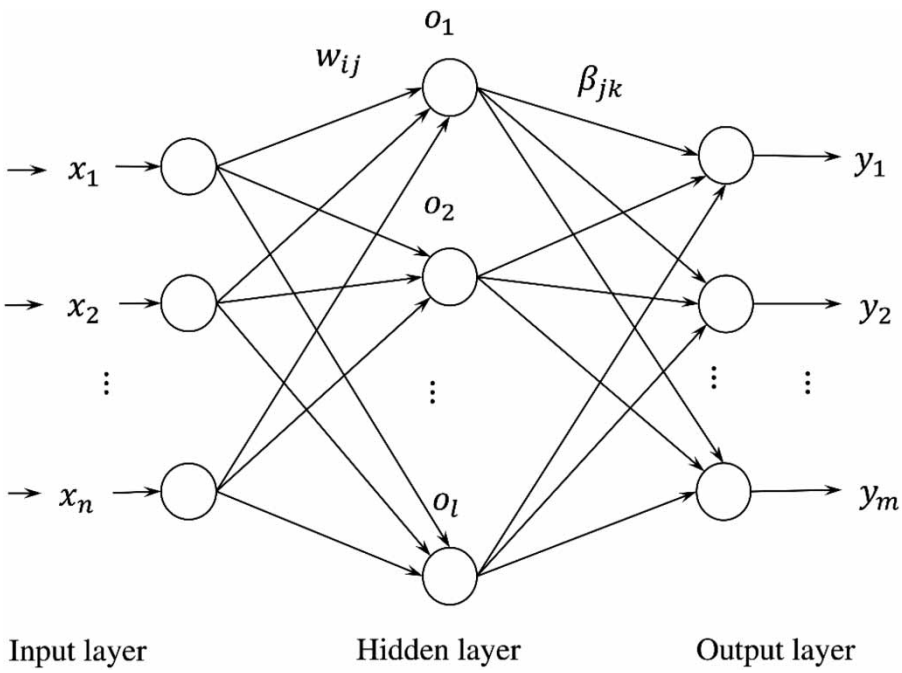

Figure 2 | Structure of the ELM.

used. Thus, the ELM could be shown as $H\beta = T^T$ where H is defined as:

$$H = \begin{bmatrix} g(w_1x_1 + b_1) & g(w_2x_1 + b_2) & \cdots & g(w_lx_1 + b_l) \\ g(w_1x_2 + b_1) & g(w_2x_2 + b_2) & \cdots & g(w_lx_2 + b_l) \\ \vdots & \vdots & & \vdots \\ g(w_1x_Q + b_1) & g(w_2x_Q + b_2) & \cdots & g(w_lx_Q + b_l) \end{bmatrix}_{Q\times l} \quad (4)$$

The results of ELM are exact when the number of neurons in the hidden layer (l) are equal to the number of problem samples (Q). However, this model is very big and probably trapped in the over-fitting. So that l is always considered to be much lower than Q and the model has an error that is defined by $\sum_{j=1}^{Q} ||t_j - y_j|| < \varepsilon$ where ϵ is always bigger than zero.

In the ELM training, after selecting w and b randomly, the β matrix is obtained by using the $\min_{\beta} ||H\beta - T^T||$ where H^+ is the Moore-Penrose generalized inverse matrix of H. The solution of this equation is obtained by $\hat{\beta} = H^+T^T$. In the present study, the trial and error method is employed in order to determine the hidden layer's neuron number.

Differential evolution

The DE optimization algorithm is introduced by Storn & Price (1997) as a global search method for optimizing the network parameters. This algorithm has a high convergence speed and automatic exploration-exploitation adjustability. The goal of DE is to minimize the objective function $f(\theta)$ where θ is the parameter vector. In searching for the optimum solution, the DE generates N_p populations. At the Gth generation, the ith parameter vector is written as:

$$\theta_{i,G} = [\theta^1_{i.G}, \theta^2_{i.G}, \ldots, \theta^D_{i.G}] \text{ where } i = 1, 2, \ldots, N_P \quad (5)$$

The DE algorithm is presented completely in Suribabu (2010). However, the main steps of this algorithm are presented briefly here.

(1) Initialization of problem: A number N_P parameter vectors $\theta_{i,G}$ are generated randomly through the following equation:

$$\theta_{i,G} = \theta_{\min} + \text{rand}(0, 1).(\theta_{\max} - \theta_{\min}) \text{ where } \begin{cases} \theta_{\min} = [\theta^1_{\min}, \theta^2_{\min}, \ldots, \theta^D_{\min}] \\ \theta_{\max} = [\theta^1_{\max}, \theta^2_{\max}, \ldots, \theta^D_{\max}] \end{cases} \quad (6)$$

In this equation, $\theta_{\min}$ and $\theta_{\max}$ are the bounds of the considered parameters.

(2) Mutation: There are various mutation strategies (Storn & Price 1997) that can be applied to produce mutant vector $v_{i,G}$ for each individual parameter vector $\theta_{i,G}$. While there are many mutation strategies, four shall be utilized:

Strategy 1:

$$v_{i,G} = \theta_{r^i_1,G} + F.(\theta_{r^i_2,G} - \theta_{r^i_3,G}) \quad (7)$$

Strategy 2:

$$v_{i,G} = \theta_{r^i_1,G} + F.(\theta_{\text{best},G} - \theta_{r^i_1,G}) + F.(\theta_{r^i_2,G} - \theta_{r^i_3,G}) + F.(\theta_{r^i_4,G} - \theta_{r^i_5,G}) \quad (8)$$

Strategy 3:

$$v_{i,G} = \theta_{r^i_1,G} + F.(\theta_{r^i_2,G} - \theta_{r^i_3,G}) + F.(\theta_{r^i_4,G} - \theta_{r^i_5,G}) \quad (9)$$

Strategy 4:

$$v_{i,G} = \theta_{i,G} + F.(\theta_{r^i_1,G} - \theta_{i,G}) + F.(\theta_{r^i_2,G} - \theta_{r^i_3,G}) \quad (10)$$

where r^i_k are integers obtained randomly within the range [1, 2, ..., N_P] interval. The first two strategies are suitable for solving multi-modal problems with strong exploration capacity. However, they demonstrate slow convergence speed and sometimes get stuck at local optimum. The third and fourth strategies lead to better perturbation with an associated computation cost.

(3) Crossover: The crossover procedure is performed on the mutated vectors to increase mutant vectors' diversity. At generation G, for each mutant vector $v_{i,G} = [v^1_{i.G}, v^2_{i.G}, \ldots, v^D_{i.G}]$ a trial vector of $u_{i,G} = [u^1_{i.G}, u^2_{i.G}, \ldots, u^D_{i.G}]$ is generated

using the crossover as follows:

$$u_{i,G}^{j} = \begin{cases} v_{i,G}^{j}, & \text{if}(\text{rand}_j \le CR) \quad \text{or} \quad (j = j_{\text{rand}}) \\ \theta_{i,G}^{j}, & \text{Otherwise} \end{cases} \tag{11}$$

In the above equation, CR is the crossover coefficient used to control the fraction of the parameters copied from mutant vector and has the value between 0 and 1. The j_{rand} is a random integer with value between 1 to D that is used in order to ensure that at least one of the $u_{i,G}$ parameters is different from $\theta_{i,G}$.

(4) Selection: This is the final step in the DE algorithm that is used to find the individual vectors with minimum error according to a defined fitness function. Steps (2) to (4) are repeated to reach the defined precision or the maximum number of iterations.

SAELM method

The SAELM method utilized in this study is a self-adaptive ELM method that employs the evolutionary DE (Cao *et al.* 2012). In the SAELM method, the self-adaptive DE is utilized to determine the input weights and hidden node biases, while the ELM method is used to develop the output weights. Initially, the self-adaptive DE algorithm is used to generate random N_P vectors as populations in the first generation, $\theta_{k,G} = [a_{1,(k,G)}^T, \cdots, a_{L,(k,G)}^T, b_{1,(k,G)}, \cdots, b_{L,(k,G)}]$.

The output weight matrix is determined by the equation of $\beta_{k,G} = H_{k,G}^{-1}T$, where $H_{k,G}^{-1}$ = the generalized inverse of $H_{k,G}$ and can be written as:

$$H_{k,G} = \begin{bmatrix} g(a_{1,(k,G)}, b_{1,(k,G)}, x_1) & \cdots & g(a_{L,(k,G)}, b_{L,(k,G)}, x_1) \\ \vdots & \ddots & \vdots \\ g(a_{1,(k,G)}, b_{1,(k,G)}, x_N) & \cdots & g(a_{L,(k,G)}, b_{L,(k,G)}, x_N) \end{bmatrix} \tag{12}$$

In addition, the root mean square error ($RMSE$) of each individual is calculated as:

$$RMSE_{k,G} = \sqrt{\frac{\sum_{i=1}^{N} \left| \sum_{j=1}^{L} \beta_j g(a_{j,(k,G)}, b_{j,(k,G)}, x_i) - t_i \right|}{m \times N}} \tag{13}$$

The population vector with the best $RMSE$ is stored in the first generation. In subsequent generations, the parameter vectors are evaluated using the following equation:

$$\theta_{k,G+1} = \begin{cases} u_{k,G+1} & \text{if } RMSE_{\theta_{k,G} - RMSE_{\theta_{k,G+1}} > \varepsilon . RMSE_{\theta_{k,G}}} \\ u_{k,G+1} & \text{if } |RMSE_{\theta_{k,G}} - RMSE_{\theta_{k,G+1}}| < \varepsilon . RMSE_{\theta_{k,G}} \\ & \quad \text{and} \quad |\beta_{u_{k,G+1}}| < |\beta_{\theta_{k,}}| \\ \theta_{k,G} & \text{else} \end{cases} \tag{14}$$

In the utilized self-adaptive DE algorithm, the trial vector is generated for each target vector by using one of the previous four strategies.

The strategy choice at each generation is done according to a probability procedure $P_{l,G}$. The $P_{l,G}$ is the probability that the lth strategy is selected in the Gth generation. In the developed model l can be 1, 2, 3 or 4. The $P_{l,G}$ is updated such that if G is less than or equal to P (number of generated vectors in each population), the four considered strategies have equal probabilities and $P_{l,G} = 0.25$. Else, if G is bigger than P then $P_{l,G}$ is obtained from the following equation:

$$P_{l,G} = \frac{S_{l,G}}{\sum_{l=1}^{4} S_{l,G}} \text{ where } S_{l,G} = \frac{\sum_{g=G-P}^{G-1} ns_{l,g}}{\sum_{g=G-P}^{G-1} ns_{l,g} + \sum_{g=G-P}^{G-1} nf_{l,g}} + \varepsilon \tag{15}$$

where $nf_{l,g}$ = number of trial vectors generated by the lth strategy at gth generation that are successfully entered in the coming generations, $ns_{l,g}$ = number of trial vectors generated by the lth strategy at gth generation that are discarded from the coming generations, ε = a positive constant to prevent the zero improvement rate. The F and CR parameters are chosen for each target vector by selection from normally distributed functions. The generation of the trial vectors for the next generation is done by using the $\theta_{\text{k,G+1}}$ equation that is presented before. In the SAELM method, evolution continues until the required fitness is achieved.

Multi-layer perceptron neural network

Multi-layer ANN has been widely used in the engineering fields, because of the flexibility of this method in solving the nonlinear problems. ANN structure has three layers of input, hidden, and output. The problem's input variables

are introduced to the network by using the input layer's neurons. The results of the neural network are obtained from the output layer's neuron. The weights and biases of each neuron are determined using the back propagation algorithm. The hidden layer's neurons calculate the weighted summation of the input layer's neurons and place the result in the transfer function. There are many transfer functions that could be used for the hidden layer's neurons. However, the hyperbolic tangent (Equation (16)) is very common (Zadeh *et al.* 2010; Emiroglu *et al.* 2011; Pierini *et al.* 2012).

$$\text{tansig}(n) = \frac{2}{1+e^{-2n}} - 1 \tag{16}$$

The input and output layer neurons numbers are equal to the input and output variables of the problem, respectively. However, there is not a definitive rule to determine the hidden layer's neurons number. In the present study, trial and error is utilized in order to select the appropriate number of hidden neurons. More details of the ANN algorithm are given in Karunanithi *et al.* (1994) and Haykin (2004).

Support vector machines

One of the supervised learning methods in the fields of regression and classification is SVM (Vapnik *et al.* 1996; Huang *et al.* 2002). Unlike the other neural networks that are performed from local training errors in their training process, the SVM method uses the upper band generalization error minimization in its training procedure (Shamshirband *et al.* 2015). The detailed description of SVM is presented in Rajasekaran *et al.* (2008) and Yang *et al.* (2009). In the present study, the RBF kernel function (Jahangirzadeh *et al.* 2014; Ebtehaj *et al.* 2016) that has a satisfactory result is used in order to handle the modeling procedure. The RBF kernel function is defined as follows:

$$K(x_i, x_j) = \exp\left(-\gamma ||x_i - x_j||^2\right) \tag{17}$$

Error performance indicators

Once the SAELM models are developed, they are tested against the following statistical error indicators. These error measures are the mean absolute relative error (*MARE*), *RMSE* and scatter index (*SI*). They are defined as:

$$MARE = \frac{1}{n}\sum_{i=1}^{n}\left(\frac{|(d_s/y)_{\text{observed } i} - (d_s/y)_{\text{Predicted } i}|}{(d_s/y)_{\text{observed } i}}\right) \tag{18}$$

$$RMSE = \frac{1}{n}\sum_{i=1}^{n}((d_s/y)_{\text{observed } i} - (d_s/y)_{\text{Predicted } i})^2 \tag{19}$$

$$SI = \frac{RMSE}{\sum_{i=1}^{n}(d_s/y)_{\text{observed } i}} \tag{20}$$

RESULTS AND DISCUSSION

Pier scour dataset

The local pier scour dataset used in this study is collected from actual field datasets (Landers & Mueller 1999; Mohammed *et al.* 2005) and consists of 476 measurements. These measurements are for pier local scour collected from 14 different sites in Pakistan, India and Canada. Besides being field measurements, the dataset has the advantage of including four different shapes of bridge piers: sharp, square, round and cylindrical. The measured dataset includes the flow velocity, depth, bed grain median diameter, bed-sediment coefficient of uniformity and pier dimensions. The pier scour dataset includes a wide range of piers classified as narrow, wide, and intermediate. According to Melville & Sutherland (1998), the flow shallowness ratio y/D can be used for pier classification, where wide piers have values of less than 0.2, and narrow piers have values greater than 1.4. In the case of narrow piers, the scour depth occurs at the upstream face of the pier, while it occurs near the pier sides on wide piers. These data have been grouped into the five effective dimensionless parameters for estimating pier local scour defined as: d_s/y, F_r, d_{50}/y, D/y, L/y and σ, where d_s is scour depth, y is flow depth, F_r is the Froude number, d_{50} is the median diameter of particle size, L is the pier length, hidden nodes and σ is the standard deviation bed

grain size parameter. The correlation between various variables and the measured pier scour is found to be very low with an average value of 0.3 implying a strong non-linear relation between them and the scour depth. This is further confirmed by examining the surface plot of pier local scour and various inputs (Figure 3). Statistical measures and ranges of various dimensionless parameters are presented in Table 2.

SAELM model development

For model development, available data are divided into training and testing datasets, 80% for training and 20% for testing. Training and testing datasets are chosen randomly such that the statistical measures for both subsets are close. Various combinations (Figure 4) of input variables are used to test the SAELM model sensitivity to inputs. Depending on the number of variables used to develop the SAELM model, the developed models are grouped into five categories, C1, C2, C3, C4, and C5. C1 is a SAELM model developed with only one variable, C2 is a SAELM model developed with only 2 variables and so on.

The developed SAELM model has the following simple general form:

$$\frac{d_s}{y} = \left[\frac{1}{(1+\exp(InW \times InV + BHI))}\right]^T \times OutW \tag{21}$$

where InV is the input variable vector having dimension of (1×1) for C1 models and (5×1) for C5 models, BHI is the bias of the hidden neuron vector, InW is the input weight matrix, and $OutW$ is the output weight vector. These vectors and matrices are determined through an optimization process using the DE algorithm within the SAELM

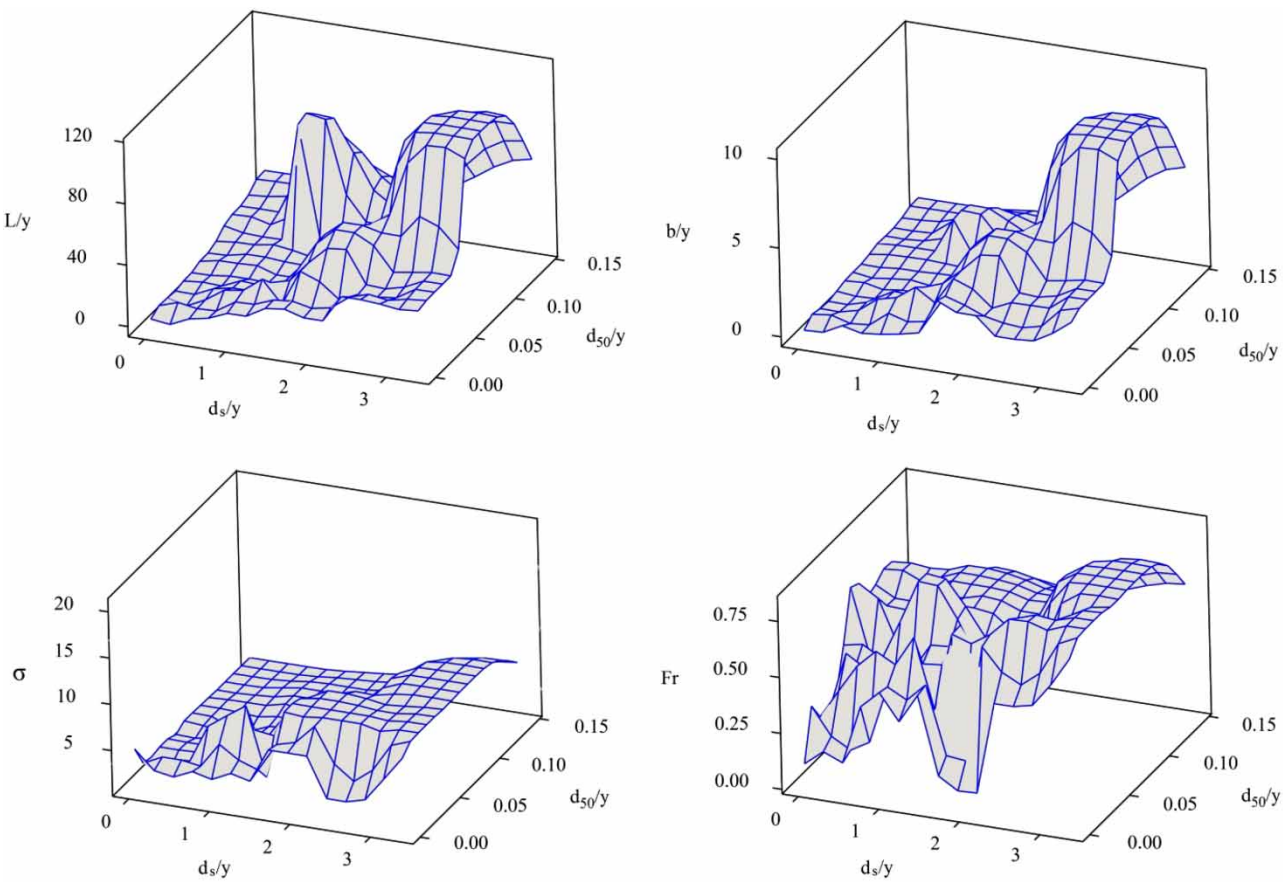

Figure 3 | Surface plots of various dimensionless parameters versus measured local pier scour.

Table 2 | Statistical measures for various dimensionless parameters for each pier shape

			Dimensionless variable					
Statistical parameter	**Pier shape**	**Data number**	d_s/y	Fr	d_{50}/y	D/y	L/y	σ
Maximum	Sharp	95	3.30	0.82	0.10	10.00	110.00	14.00
	Round	231	2.00	0.61	0.14	3.00	25.00	20.00
	Square	107	2.50	0.58	0.00	1.50	37.00	6.20
	Cylindrical	43	0.74	0.45	0.00	2.70	44.00	6.90
Minimum	Sharp	95	0.03	0.05	0.00	0.20	0.45	1.20
	Round	231	0.00	0.03	0.00	0.09	0.00	1.30
	Square	107	0.00	0.03	0.00	0.04	0.52	1.80
	Cylindrical	43	0.05	0.03	0.00	0.10	0.62	1.90
Average	Sharp	95	0.51	0.35	0.02	0.80	10.00	3.60
	Round	231	0.24	0.23	0.01	0.45	4.20	3.20
	Square	107	0.35	0.21	0.00	0.38	5.40	3.00
	Cylindrical	43	0.22	0.16	0.00	0.39	2.70	4.00
SD	Sharp	95	0.35	0.04	0.00	1.50	250.00	6.70
	Round	231	0.13	0.03	0.00	0.30	47.00	7.90
	Square	107	0.16	0.04	0.00	0.28	72.00	2.10
	Cylindrical	43	0.11	0.05	0.00	0.36	100.00	5.40
CV	Sharp	95	0.68	0.11	0.03	1.90	25.00	1.80
	Round	231	0.53	0.11	0.07	0.66	11.00	2.40
	Square	107	0.46	0.19	0.58	0.73	13.00	0.68
	Cylindrical	43	0.49	0.32	0.49	0.91	37.00	1.40

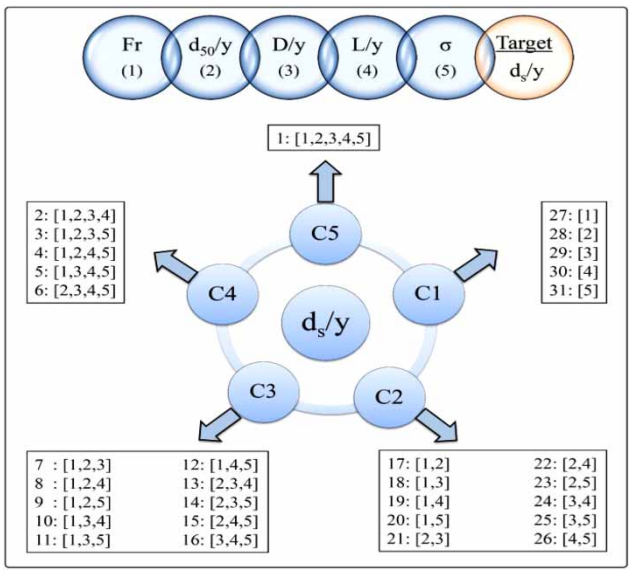

Figure 4 | Combinations of input parameters used to develop SAELM model.

framework based on the number of chosen input variables. For example, the optimized *InV*, *BHI*, *OutW* vectors and *InW* matrix for SAELM model C5 are written as:

$$InV = \begin{bmatrix} Fr \\ \frac{d_{50}}{y} \\ \frac{D}{y} \\ \frac{L}{y} \\ \sigma \end{bmatrix} \quad BHI = \begin{bmatrix} -1.79 \\ 0.88 \\ -1.25 \\ 0.67 \\ -0.37 \\ -0.9 \\ 0.69 \\ 0.19 \end{bmatrix} \quad OutW = \begin{bmatrix} 3.95 \\ 1.49 \\ -0.12 \\ -0.02 \\ -0.46 \\ 1.24 \\ -1.34 \\ -0.8 \end{bmatrix} \quad InW$$

$$= \begin{bmatrix} 0.53 & 0.36 & 0.38 & 0.01 & -0.03 \\ -0.55 & -3.57 & -0.17 & -0.08 & 0.5 \\ 1.11 & 1.2 & -0.31 & 1.62 & 0.14 \\ -0.99 & -0.69 & 0.84 & 0 & -0.84 \\ -0.42 & 0.29 & 0.33 & -0.37 & 0.51 \\ -0.61 & -0.17 & -0.53 & 0.33 & -0.33 \\ -0.53 & 0.5 & 0.37 & 0.04 & 1.23 \\ -1.16 & -0.55 & -0.51 & 0.57 & -0.51 \end{bmatrix}$$

The choice of the best SAELM model can be made based on the score in the previously mentioned error indicators such as *MARE* together with the SI. Figure 5 shows the SAELM model scores in *MARE* and *SI* indicators for all 30 models with various numbers of input variables. Using four input variables, the developed SAELM models show similar performance except for model 2, which utilizes *Fr*, *D/y*, *L/y* and d_{50}/y as input variables. This model has the highest *MARE* and *SI* (*MARE* = 1.68, *SI* = 1.61) that is four times higher than other models. Absence of the sediment standard deviation seems to have a significant impact on the accuracy of prediction of scour depth. The inclusion of d_{50}/y in models 3, 4 and 6 obtained equal performance for the SAELM models irrespective of adding or removing *L/y* and *Fr*. The minimum error was obtained for the SAELM model with *MARE* of 0.44 for SAELM model number 5. The optimized parameters of the SAELM model number 5 (function of *Fr*, *D/y*, *L/y* and σ) are

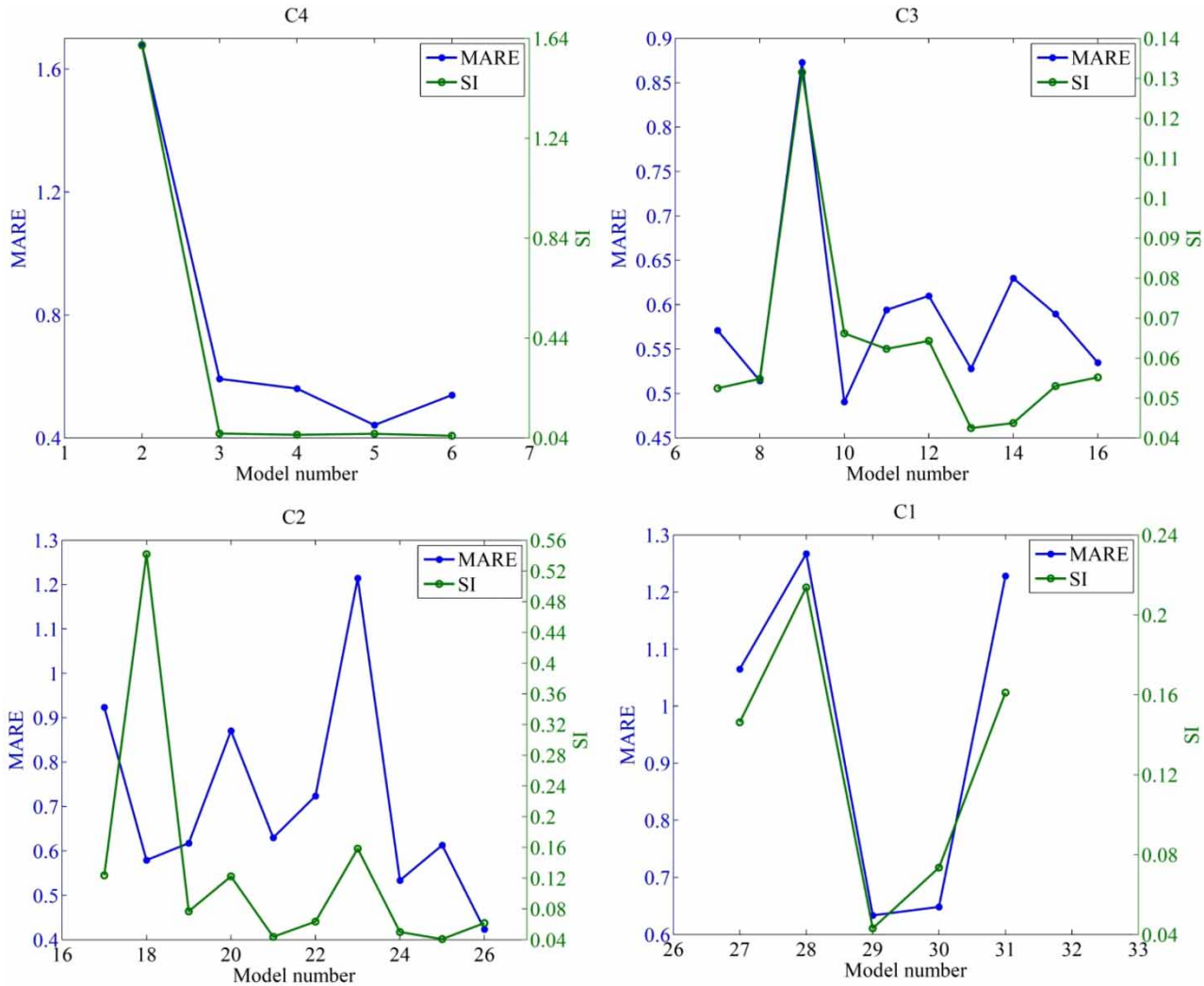

Figure 5 | Performance evaluation of developed SAELM models.

written as:

$$InV = \begin{bmatrix} Fr \\ \frac{D}{y} \\ \frac{L}{y} \\ \sigma \end{bmatrix} \quad BHI = \begin{bmatrix} 0.94 \\ -0.2 \\ -0.53 \\ 1.98 \\ -6.45 \\ -1.56 \\ -0.77 \\ -5.32 \\ 1.88 \\ -0.49 \\ 0 \\ -0.81 \\ -0.12 \\ 1.42 \\ 2.63 \\ 2.66 \end{bmatrix} \quad OutW = \begin{bmatrix} 0.72 \\ -0.53 \\ -2.02 \\ -0.56 \\ 0.55 \\ 0.18 \\ -0.41 \\ 0.18 \\ 0.24 \\ 3.55 \\ -1.3 \\ -1 \\ 0.15 \\ 0.27 \\ -2.67 \\ 1.62 \end{bmatrix}$$

$$InW = \begin{bmatrix} 0.14 & 0.84 & -1.18 & -0.38 \\ 1.99 & -1.91 & -0.91 & 0.06 \\ 0.94 & -0.58 & 0.07 & -0.69 \\ -1.03 & 1.83 & -0.78 & 0.7 \\ -2.31 & 1.18 & 0.27 & -0.14 \\ -1.01 & 1.64 & -0.85 & 0.15 \\ -0.93 & 0.5 & -0.18 & 0.49 \\ 1.39 & -0.95 & 0.14 & 0.92 \\ 0.04 & 0.42 & -0.88 & 0.44 \\ 0.56 & 0.06 & 0.02 & 0 \\ -0.14 & -0.26 & -0.79 & -0.99 \\ -0.62 & 1.87 & 0.95 & 0.62 \\ -1.21 & -0.51 & 1.82 & 0.68 \\ 1.75 & 2.01 & -0.28 & -0.03 \\ 0.94 & -1.2 & -1.19 & -2.14 \\ 0.74 & -0.65 & -0.37 & -2.35 \end{bmatrix}$$

Results of SAELM models in category C3 show higher error than category C4 models. This is probably due to the inclusion of only three input variables. The worst predictions were obtained for model number 9 with $MARE = 0.87$ and $SI = 0.13$. Model number 9 did not include D/y and L/y as input variables, which implies that they are important predictors that have to be included in scour depth prediction model development. The pier shape characteristics parameters (i.e. pier length L and pier width D) are considered as effective dimensionless parameters (D/y and L/y) that must be used in scour depth prediction. Excluding either of them (models number 3 and 4) or both (model 9) significantly reduced the accuracy of scour depth prediction.

Among the models with three different input variables (in category C3), in the case where parameters Fr and d_{50}/y are fixed (C3 (7), C3 (8), C3 (9)) the best performance is obtained when the L/y is used as a third control variable. This was achieved in model number 8 with $MARE = 0.51$ and $SI = 0.055$. In the third category, the best models with least error are model numbers 10 and 13. Error and scatter indices are $MARE = 0.49$, $SI = 0.066$, and $MARE = 0.53$, $SI = 0.043$ for models number 10 and 13, respectively. The similarities between these two models is the use of both of dimensionless parameters of pier shape characteristics (L/y and D/y). The usage of these parameters with Froude number (Fr) or dimensionless parameter of median diameter of particle size (d_{50}/y) simultaneously, resulted in the best input combinations in scour depth prediction model development. The optimized parameters of the SAELM model number 10 (function of Fr, D/y, L/y) are written as:

$$InV = \begin{bmatrix} Fr \\ \frac{D}{y} \\ \frac{L}{y} \end{bmatrix} \quad BHI = \begin{bmatrix} -3.03 \\ -1.83 \\ -4.84 \\ 1.25 \end{bmatrix} \quad OutW = \begin{bmatrix} 0.37 \\ 1.99 \\ 0.65 \\ -0.24 \end{bmatrix}$$

$$InW = \begin{bmatrix} -0.24 & 0.1 & 0.09 \\ 0.85 & 0.99 & -0.04 \\ -0.12 & -0.96 & 0.55 \\ -0.06 & 0.35 & 0.72 \end{bmatrix}$$

The SAELM models with two input variables are presented in category C2. Within the models that use Fr as one of the two input variables, considering the bridge pier shape characteristics (D/y or L/y) lead to best results so that the $MARE$ of SAELM models number 18 and 19 are 0.58 and 0.62, respectively. By considering flow velocity as Fr and bridge pier shape characteristics as D/y or L/y, the results of these input combination lead to good results relative to SAELM models 17 and 20. Within the category C2 with two input variables, SAELM models number 25 and 26 provided the best

results with the least error. Both models are a function of the sediment standard deviation in addition to either L/y or D/y. The optimized parameters of the SAELM models number 25 and 26 (function of σ, D/y or L/y) are written as:

$$InV = \begin{bmatrix} \frac{D}{y} \\ \sigma \end{bmatrix} \quad BHI = \begin{bmatrix} -0.66 \\ -3.35 \end{bmatrix} \quad OutW = \begin{bmatrix} 0.26 \\ 2.26 \end{bmatrix}$$

$$InW = \begin{bmatrix} 5.87 & -0.68 \\ 1.31 & 0.05 \end{bmatrix}$$

and

$$InV = \begin{bmatrix} \frac{L}{y} \\ \sigma \end{bmatrix} \quad BHI = \begin{bmatrix} 0.27 \\ -2.35 \\ 3.26 \\ 0.28 \\ -1.81 \end{bmatrix} \quad OutW = \begin{bmatrix} -2.29 \\ 2.17 \\ 1.24 \\ 1.37 \\ 0.68 \end{bmatrix}$$

$$InW = \begin{bmatrix} 0.65 & 0.43 \\ 0 & 0.58 \\ 0.08 & -0.54 \\ 0.27 & -0.62 \\ -0.32 & 0.14 \end{bmatrix}$$

In the case of using only one control variable, SAELM models in category 1 produced higher error than models in other categories. The term D/y as a single control variable proved to be the best predictor for the scour depth around bridge piers in SAELM model number 29 with $MARE = 0.63$ and $SI = 0.043$.

Selecting the best SAELM models in all categories is based on their low scores in *MARE* and *SI*. The best models in each of the SAELM categories (C1 to C4) are shown in Figure 6. It can be finally concluded that model number 13 in category C3 can be selected as the best optimum SAELM model ($MARE = 0.53$ and $SI = 0.042$) for prediction of scour depth around bridge piers. This model utilizes the ratio of median diameter of particle size to flow depth (d_{50}/y), ratio of pier length to flow depth (L/y) and ratio of pier width to flow depth (D/y) as predictors. These three parameters have been confirmed by Melville & Sutherland (1998) as being the most important parameters affecting the scour process. The parameters L/y and D/y represent the effects of the depth of flow in relation to the pier dimensions and are of utmost importance in the formation of the scour hole. For deep flow, the scour depth increases in proportion to pier width since the horseshoe vortex and associated downflow are related to the pier width. In the case of shallower flows (high values of L/y and D/y), a surface roller is formed on the surface and become more dominant making the bass vortices less capable to entrain sediment. For intermediate flows, the scour depth becomes a function in both flow depth and pier dimensions.

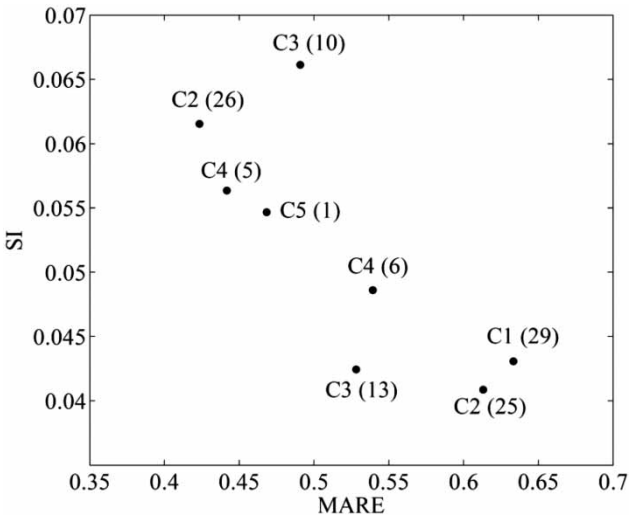

Figure 6 | Selection of best SAELM model.

Comparison of the SAELM models with existing regression models

Using the chosen SAELM model, the relative scour depth d_s/y as predicted by model is drawn versus observed values for four shapes of bridge piers as shown in Figure 7. SAELM model predictions are plotted in addition to regression-based models of Laursen & Toch (1956), Shen *et al.* (1969), Johnson (1992) and Richardson & Davis (2001). In general, the scatter of predictions away from the perfect fit line is observed to be higher in the case of regression-based models compared to SAELM model. In the cases of sharp, round and cylindrical bridge piers, all regression-based models over-predicted the scour depth with three orders of magnitude except for Johnson (1992) model, which underestimated the scour depth with two orders of magnitude. SAELM model predictions are observed to be balanced with respect to estimation of scour depth with less error than other available models. This is

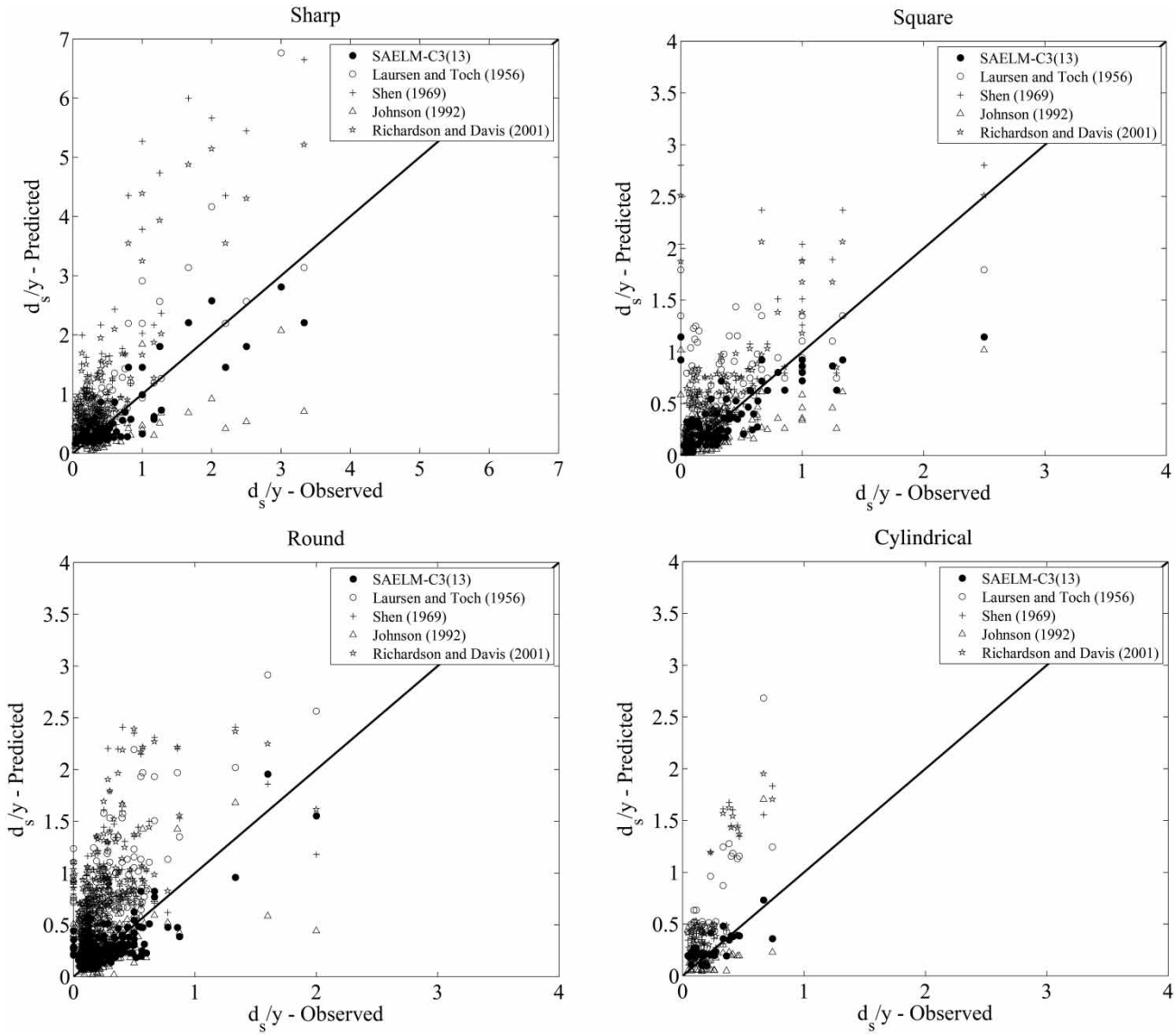

Figure 7 | Comparison of SAELM with existing regression-based equations.

confirmed with results shown in Table 3 that compares error estimates of SAELM and available regression-based models. The SAELM-C3(13) model produced the best results with lowest $RMSE = 0.0283$ and $MARE = 0.719$. This superior prediction capability is observed for all shapes of bridge piers.

Moreover, Figure 8 shows the dimensionless scour depth as calculated by the developed SAELM model and some of the traditional regression-based models versus the non-dimensional pier width, D/y. This parameter has been chosen since it represents the most important parameter controlling the pier sour hole size and characteristics (Melville 1988; Melville & Coleman 2000). It is shown that the model predictions of Laursen & Toch (1956), Shen *et al.* (1969), and Richardson & Davis (2001) gave similar values for the scour depth versus the non-dimensional pier width D/y. These predictions showed larger values than Johnson (1992) and SAELM models, which had close values. The SAELM model showed similar trend of predictions with available models, where the predicted non-dimensional scour depth increased in a linear manner with the increase in the non-dimensional pier width. The most important length scale that affects the scour process

Table 3 | Statistical index for SAELM and existing regression-based equations

Statistical index	Pier shape	SAELM-C3(13)	Laursen & Toch (1956)	Shen *et al.* (1969)	Johnson (1992)	Richardson & Davis (2001)
RMSE	Sharp	0.283	0.729	1.678	0.509	1.285
	Round	0.142	0.567	0.634	0.230	0.652
	Square	0.251	0.460	0.488	0.336	0.474
	Cylindrical	0.112	0.536	0.514	0.216	0.538
MARE	Sharp	0.719	2.649	3.046	0.958	3.160
	Round	0.555	2.703	2.517	0.539	2.867
	Square	0.597	2.154	1.281	0.793	1.756
	Cylindrical	0.540	2.532	1.540	0.675	2.013

The underlined values in this table show the lowest values for *RMSE* and *MARE* on different pier shape for SAELM-C3(13) method when compared with other methods.

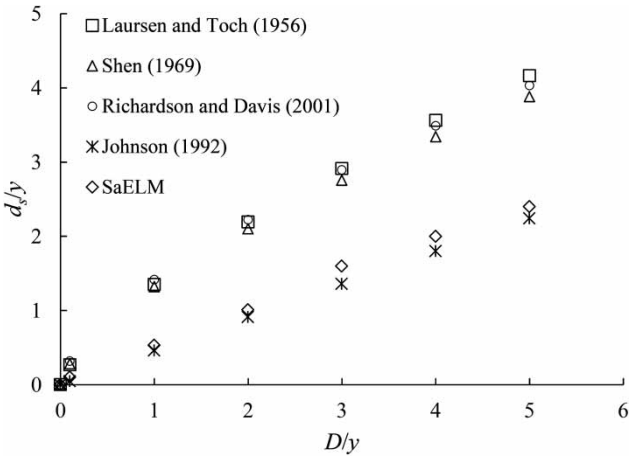

Figure 8 | Scour depth prediction of SAELM model and available traditional equations versus non-dimensional pier width.

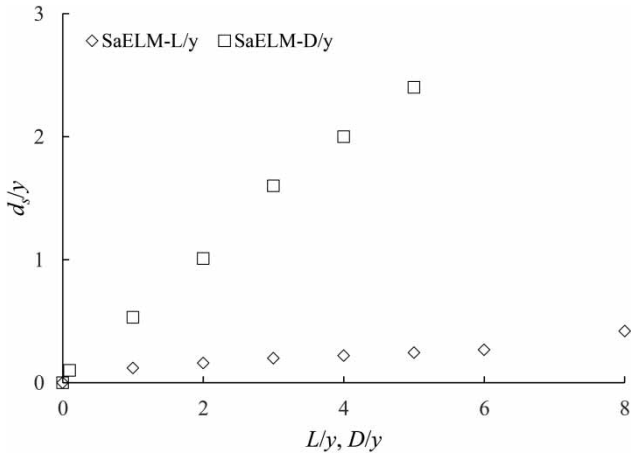

Figure 9 | Scour depth prediction of SAELM model versus non-dimensional pier width and length.

has been reported to be the pier dimension, where it has a direct impact on the formed vortex intensity and the coherent turbulent structure (Melville & Coleman 2000). The increase in the pier width leads to a proportional increase in the scour hole depth until the ratio of y/D reaches 1.4 (Melville 1988), where the pier becomes narrow and the scour hole depth responds slowly to the change in pier dimension. The pier width has been stated to have more influence on scour hole depth, than pier length (Melville 1988). This is very obvious in the SAELM model predictions shown in Figure 9. This figure shows that the non-dimensional scour depth d_s/y increases linearly with the increase in pier dimension. It shows also a higher influence of the pier width over the pier length. For example, the increase in pier width D/y from 2 to 4 leads to an increase in scour depth d_s/y from 1 to 2, while the same increase in pier length L/y from 2 to 4 leads to a corresponding increase in scour depth d_s/y from 0.1 to 0.25. This has been confirmed by the experimental measurements of Laursen & Toch (1956), Raudkivi (1986) and Ettema *et al.* (1998), among others. This is attributed to the strength of the horseshoes vortex and associated down flow, which is a main cause of the pier scour. The strength of this vortex is directly proportional to the transversal direction of the pier rather than its length, where the latter has little influence (Melville 1988). A sediment coarseness parameter has been defined (Melville 1988) to characterize the bed sediment and quantify its impact on the extent of scour hole in front of piers. It was defined as the pier width divided by the median bed grain size D/d_{50}. Figure 10 shows the non-dimensional

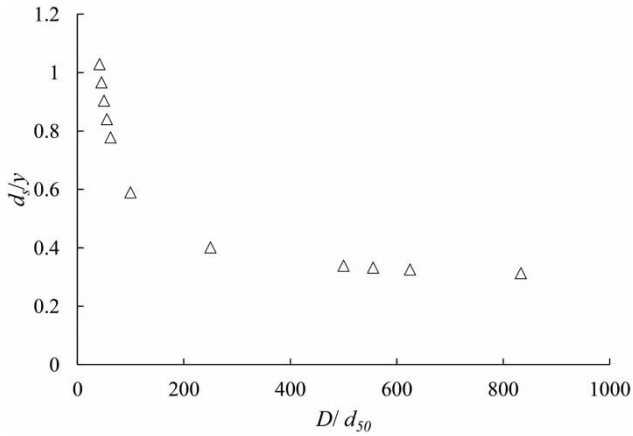

Figure 10 | Scour depth prediction of SAELM model versus sediment coarseness.

scour depth as predicted by the SAELM model versus the sediment coarseness parameter D/d_{50}. The data collected have a minimum value of sediment coarseness parameter of 41, which is close to the limit value of 50 that defines a 'fine' sediment bed (Ettema *et al.* 1998). For this range, $D/d_{50} \geq 50$, the scour depth is inversely proportional to the sediment coarseness. This trend has also reported in experimental measurements of Sheppard & Glasser (2004). As the sediment coarseness increases, the bed particle diameter decreases, this changes the physical behavior of the sediment bed. Therefore, the inter-particle cohesion increased and the scour depth decreased.

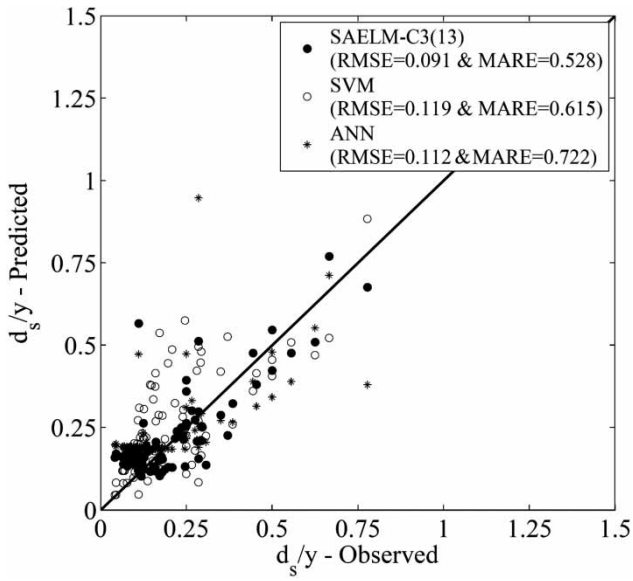

Figure 11 | Comparison of SAELM with SVM and ANN for predicting scour depth.

Comparison of the SAELM models with ANN and SVM

The performance of SAELM in predication of scour depth around bridge pier was compared with SVM and ANN in Figure 11. The ANN approach predicted the d_s/y with high level of errors ($MARE = 0.722$ and $RMSE = 0.112$) especially for $d_s/y > 0.35$. The statistical indices ($MARE = 0.615$ and $RMSE = 0.119$) related to SVM showed higher accuracy than ANN but still not as good as the SAELM model. In general, Figure 11 shows the SAELM (C3)13 has better performance than other machine-learning methods with respect to the calculated error and prediction scatter.

Uncertainty analysis for the SAELM model predictions

In this section, a quantitative assessment of the uncertainties in the prediction of the pier scour depth is presented using the developed SAELM model versus the regression-based models and ANN, and SVM models. The uncertainty analysis is applied to the test data used in this study (Sattar 2016; Sattar *et al.* 2016). While using this set might give advantage to the developed SAELM model, it will also present a fair comparison to show the uncertainties in predictions of various equations when applied to field data. The uncertainty analysis defines the individual prediction error as $e_j = P_j - T_j$. The calculated prediction errors for the entire dataset are used to calculate the mean and standard deviation of the prediction errors as $\bar{e} = \sum_{j=1}^{n} e_j$ and $S_e = \sqrt{\sum_{j=1}^{n} (e_j - \bar{e})^2 / n - 1}$, respectively. A negative mean value indicates that the prediction model underestimated the observed values, and a positive value indicates that the

Table 4 | Uncertainty analysis for SAELM model versus others

Model	No. of samples	Mean prediction error	Width of uncertainty band	95% prediction error interval
SAELM	476	+0.004	±0.03	−0.02 to +0.03
Laursen & Toch (1956)	476	+0.46	±0.05	+0.41 to +0.52
Shen *et al.* (1969)	476	+1.01	±0.14	+0.87 to +1.16
Johnson (1992)	476	−0.16	±0.09	−0.24 to −0.07
Richardson & Davis (2001)	476	+0.87	±0.10	+0.77 to +0.97

equation overestimated the observed values. Using the values of $\bar{e}$ and S_e, a confidence band can be defined around the predicted values of an error using Wilson score method without continuity correction; the use of $\pm 1.96\ S_e$ yields an approximately 95% confidence band. Table 4 summarizes the results of the uncertainty analysis, and shows the mean prediction errors of the various models, the width of the uncertainty band and the 95% prediction interval error.

It is observed that the developed SAELM model has performed better than available regression models with less calculated uncertainty. The absolute mean error of prediction for the SAELM model is calculated as +0.004 compared to +0.46 to +1.01 for Laursen & Toch (1956) and Shen *et al.* (1969). All models including the developed SAELM model overpredicted the pier scour depth. The regression model of Johnson (1992) had the least mean prediction error of −0.16, while Shen *et al.* (1969) had the highest mean prediction error of +1.01. The uncertainty bans for traditional regression models were close and ranged from ±0.05 to ±0.10, while that for the SAELM model was lower with a value of ±0.03. Similarly, the lowest 95% confidence prediction error interval was observed for the SAELM model. The SAELM model had the lowest mean prediction error and the smallest uncertainty bands of all the compared models.

CONCLUSIONS

This study has provided the SAELM method to develop a prediction model for scour depth around bridge piers. The SAELM model is introduced to avoid local minimum and achieve global minimum in an evolutionary procedure. Among 31 different input combination presented in this study, eight different models (i.e. models C1(29), C2(25 & 26), C3(10 & 13), C4(5 & 6) and C5(1)) which are from all categories, had similar results. The developed SAELM model is found to be the best input combination considering relative of median diameter of particle size to flow depth (d_{50}/y), relative of pier length to flow depth (L/y) and relative of pier width to flow depth (D/y) parameters (Model C3(13)). Comparing the three artificial intelligence techniques in this paper shows that SAELM ($RMSE = 0.091$ and $MARE = 0.528$) outperformed the SVM ($RMSE = 0.119$ and $MARE = 0.615$) and ANN ($RMSE = 0.112$ and $MARE = 0.722$) approaches. Comparison of the developed SAELM model with traditional regression-based models has shown the superior capability of the SAELM model, which predicted the scour depth around bridge piers with various shapes with least error and data scatter. The developed SAELM model can be utilized by practitioners to estimate relative scour depth around bridge piers for economical design.

REFERENCES

Ab Ghani, A. & Nalluri, C. 1996 Development of pier scour equations. In: *10th Congress of Asian-Pacific Division of International Association for Hydraulic Research, Langkawi, Malaysia*, pp. 295–302.

Babovic, V. 2000 Data mining and knowledge discovery in sediment transport. *Computer-Aided Civil and Infrastructure Engineering* **15**, 383–389.

Babovic, V. 2009 Introducing knowledge into learning based on genetic programming. *Journal of Hydroinformatics* **11**, 181–193.

Babovic, V., Keijzer, M. & Bundzel, M. 2000 From global to local modelling: a case study in error correction of deterministic models. In: *Proceedings of Hydroinformatics 2000*, IAHR, CDROM_EM5.

Cao, J. & Xiong, L. 2014 Protein sequence classification with improved extreme learning machine algorithms. *BioMed Research International* 12. doi:10.1155/2014/103054.

Cao, J., Lin, Z. & Huang, G. 2012 Self-adaptive evolutionary extreme learning machine. *Neural Processing Letters* **36**, 285–305.

Chiew, Y. 1984 *Local Scour at Bridge Piers*. PhD Thesis, University of Auckland, New Zealand.

Dey, S., Bose, S. & Sastry, G. 1995 Clear water scour at circular piers: a model. *Journal of Hydraulic Engineering* **121**, 869–876.

Ebtehaj, I. & Bonakdari, H. 2014 Performance evaluation of adaptive neural fuzzy inference system for sediment transport in sewers. *Water Resources Management* **28**, 4765–4779.

Ebtehaj, I., Bonakdari, H., Zaji, A. H., Azimi, H. & Sharifi, A. 2015 Gene expression programming to predict the discharge coefficient in rectangular side weirs. *Applied Soft Computing* **35**, 618–628.

Ebtehaj, I., Bonakdari, H., Shamshirband, S. & Mohammadi, K. 2016 A combined support vector machine-wavelet transform model for prediction of sediment transport in sewer. *Flow Measurement and Instrumentation* **47**, 19–27.

El-Hakeem, M. & Sattar, A. M. 2015 An entrainment model for non-uniform sediment. *Earth Surface Processes and Landforms* **40**, 1216–1226.

Emiroglu, M. E., Bilhan, O. & Kisi, O. 2011 Neural networks for estimation of discharge capacity of triangular labyrinth side-

weir located on a straight channel. *Expert Systems with Applications* **38**, 867–874.

Etemad-Shahidi, A., Bonakdar, L. & Jeng, D. S. 2015 Estimation of scour depth around circular piers: applications of model tree. *Journal of Hydroinformatics* **17**, 226–238.

Ettema, R., Mostafa, E. A., Melville, B. W. & Yassin, A. A. 1998 On local scour at skewed piers. *Journal of Hydraulic Engineering* **124**, 756–760.

Froehlich, D. C. 1988 Analysis of onsite measurements of scour at piers. In: *Proceeding of the 1988 National Conference of Hydraulic Engineering, Colorado, USA*, pp. 534–539.

Gaudio, R., Grimaldi, C., Tafarojnoruz, A. & Calomino, F. 2010 Comparison of formulae for the prediction of scour depth at piers. In: *Proceedings of 1st IAHR European Division Congress*, 4–6 May, Edinburgh, UK.

Gaudio, R., Tafarojnoruz, A. & De Bartolo, S. 2013 Sensitivity analysis of bridge pier scour depth predictive formulae. *Journal of Hydroinformatics* **15**, 939–951.

Guo, J. 2012 Pier scour in clear water for sediment mixtures. *Journal of Hydraulic Research* **50**, 18–27.

Haykin, S. 2004 *Neural Networks: A Comprehensive Foundation*. Macmillan, New York, USA.

Huang, C., Davis, L. S. & Townshend, J. R. G. 2002 An assessment of support vector machines for land cover classification. *International Journal of Remote Sensing* **23**, 725–749.

Huang, G. B., Zhu, Q. Y. & Siew, C. K. 2006 Extreme learning machine: theory and applications. *Neurocomputing* **70**, 489–501.

Huang, G. B., Zhou, H., Ding, X. & Zhang, R. 2012 Extreme learning machine for regression and multiclass classification. *IEEE Transactions on Systems, Man, and Cybernetics, Part B (Cybernetics)* **42**, 513–529.

Jahangirzadeh, A., Shamshirband, S., Aghabozorgi, S., Akib, S., Basser, H., Anuar, N. B. & Kiah, M. L. M. 2014 A cooperative expert based support vector regression (Co-ESVR) system to determine collar dimensions around bridge pier. *Neurocomputing* **140**, 172–184.

Johnson, P. A. 1992 Reliability-based pier scour engineering. *Journal of Hydraulic Engineering* **118**, 1344–1357.

Kafi, M. & Alam, J. 1995 Modification of local scour equations. *Journal of Institution of Engineers (India)* **76**, 25–29.

Karunanithi, N., Grenney, W. J., Whitley, D. & Bovee, K. 1994 Neural networks for river flow prediction. *Journal of Computing in Civil Engineering* **8**, 201–220.

Kazeminezhad, M. & Etemad-Shahidi, A. 2010 An alternative approach for investigation of the wave-induced scour around pipelines. *Journal of Hydroinformatics* **12**, 51–65.

Landers, M. N. & Mueller, D. S. 1999 U.S. Geological Survey field measurements of pier scour. In: *Compendium of Papers on ASCE Water Resources Engineering Conference 1991 to 1998*, pp. 585–607.

Laursen, E. M. & Toch, A. 1956 *Scour Around Bridge Piers and Abutments*. Iowa Highway Research Board, Ames, IA, USA, Bulletin 4.

Lian, C., Zeng, Z., Yao, W. & Tang, H. 2014 Ensemble of extreme learning machine for landslide displacement prediction based on time series analysis. *Neural Computing and Applications* **24**, 99–107.

Luo, J., Vong, C. M. & Wong, P. K. 2014 Sparse Bayesian extreme learning machine for multi-classification. *IEEE Transactions on Neural Networks and Learning Systems* **25**, 836–843.

Melville, B. W. 1988 Scour at bridge sites. In: *Civil Engineering Practice*, Vol. 2 (P. N. Cheremisinoff & N. P. Cheremisinoff, eds). Technomic Publishing, Lancaster, PA, USA, pp. 327–362.

Melville, B. W. & Coleman, S. E. 2000 *Bridge Scour*. Water Resources Publications, Highlands Ranch, CO, USA.

Melville, B. V. & Sutherland, A. J. 1998 Design method for local scour at bridge piers. *Journal of Hydraulic Engineering* **114**, 1210–1226.

Mohammed, T. H., Noor, M. J. M. M., Ghazali, A. H. & Huat, B. B. K. 2005 Validation of some bridge pier scour formulate using field and laboratory data. *American Journal of Environmental Science* **1**, 119–125.

Mueller, D. S. & Wagner, C. R. 2005 *Field Observation and Evaluations of Streambed Scour at Bridges*. Report No. FHWA–RD–03–052, US Department of Transportation, USA.

Najafzadeh, M. & Sattar, A. M. 2015 Neuro-fuzzy GMDH approach to predict longitudinal dispersion in water networks. *Water Resources Management* **29**, 2205–2219.

Pierini, J. O., Gómez, E. A. & Telesca, L. 2012 Prediction of water flows in Colorado River, Argentina/Predicción de caudales en río Colorado, Argentina. *Latin American Journal of Aquatic Research* **40**, 872.

Rajasekaran, S., Gayathri, S. & Lee, T. L. 2008 Support vector regression methodology for storm surge predictions. *Ocean Engineering* **35**, 1578–1587.

Raudkivi, A. J. 1986 Functional trends of scour at bridge piers. *Journal of Hydraulic Engineering* **112**, 1–13.

Richardson, E. V. & Davis, S. R. 2001 *Evaluating Scour at Bridges*. Hydraulic Engineering Circular No. 18 (HEC-18). US Department of Transportation, Federal Highways, Washington, DC.

Sattar, A. M. 2014 Gene expression models for prediction of dam breach parameters. *Journal of Hydroinformatics* **16**, 550–571.

Sattar, A. M. 2016 Prediction of organic micropollutant removal in soil aquifer treatment system using GEP. *Journal of Hydrologic Engineering* **04016027**, 1–15.

Sattar, A. M., Gharabaghi, B. & McBean, E. 2016 Predicting timing of watermain failure using gene expression models for infrastructure planning. *Water Resources Management* **30**, 1635–1651.

Shamshirband, S., Petkovic, D., Javidnia, H. & Gani, A. 2015 Sensor data fusion by support vector regression methodology – A comparative study. *IEEE Sensors Journal* **15**, 850–854.

Shen, H. W., Schneider, V. R. & Karaki, S. 1969 Local scour around bridge piers. *Journal of Hydraulic Division* **95**, 1919–1940.

Sheppard, D. M. & Glasser, T. 2004 Sediment scour at piers with complex geometries. In: *Proceeding of 2nd International*

Conference on Scour and Erosion, World Scientific, Singapore.

Simons, D. B. & Senturk, F. 1992 *Sediment Transport Technology: Water and Sediment Dynamics.* Water Resources Publication, CO, USA.

Storn, R. & Price, K. 1997 Differential evolution – a simple and efficient heuristic for global optimization over continuous spaces. *Journal of Global Optimization* **11**, 341–359.

Suribabu, C. 2010 Differential evolution algorithm for optimal design of water distribution networks. *Journal of Hydroinformatics* **12**, 66–82.

Tafarojnoruz, A., Gaudio, R., Grimaldi, C. & Calomino, F. 2010 Required conditions to achieve the maximum local scourdepth at a circular pier. In: *Proceedings of XXXII Convegno Nazionale di Idraulica e CostruzioniIdrauliche*, 14–17 September, Palermo, Italy.

Vapnik, V., Golowich, S. E. & Smola, A. 1996 Support vector method for function approximation, regression estimation, and signal processing. In: *10th Annual Conference on Neural Information Processing Systems, NIPS 1996, Denver, CO*, 1997, pp. 281–287.

Vojinovic, Z., Kecman, V. & Babovic, V. 2003 Hybrid approach for modeling wet weather response in wastewater systems. *Journal of Water Resources Planning and Management* **129**, 511–521.

Williams, P., Balachandar, R. & Bolisetti, T. 2013 Evaluation of local bridge pier scour depth estimation methods. In: *Proceedings of the 24th Canadian Congress of Applied Mechanics*, Saskatoon, Canada.

Yahaya, A. S. & Ab Ghani, A. 1999 Comparing bridge pier scour equations using statistical techniques. In: *Proceedings of the World Engineering Congress (WEC99)*, Kuala Lumpur, Malaysia, pp. 63–66.

Yahaya, A. S., Ab Ghani, A. & Nor Azazi, Z. 2002 Modelling bridge pier scour equations using regression methods. *Borneo Science Journal* **2**, 23–32.

Yang, H., Huang, K., King, I. & Lyu, M. R. 2009 Localized support vector regression for time series prediction. *Neurocomputing* **72**, 2659–2669.

Yu, X., Liong, S. Y. & Babovic, V. 2004 EC-SVM approach for real-time hydrologic forecasting. *Journal of Hydroinformatics* **6**, 209–223.

Zadeh, M. R., Amin, S., Khalili, D. & Singh, V. P. 2010 Daily outflow prediction by multi layer perceptron with logistic sigmoid and tangent sigmoid activation functions. *Water Resources Management* **24**, 2673–2688.

Zong, W. & Huang, G. B. 2014 Learning to rank with extreme learning machine. *Neural Processing Letters* **39**, 155–166.

First received 28 February 2016; accepted in revised form 8 September 2016. Available online 29 November 2016